Physicochem. Probl. Miner. Process., 60(6), 2024, 197068

http://www.journalssystem.com/ppmp

Physicochemical Problems of Mineral Processing

ISSN 1643-1049

Pyrite depression by sodium metabisulfite and dextrin with xanthates: contact angle, floatability, zeta potential and IR spectroscopy studies

Mario Alberto Corona-Arroyo [1], Karen López-Frías [1], Karen Solorzano [1], Cristina Echeveste[1], Ma Mercedes Salazar-Hernández [1], Kayim Pineda-Urbina [2], and Bingqiao Yang [3]

[1] Mining, Metallurgical and Geological Engineering Department, Engineering Division, Guanajuato University. Ex-Hacienda de San Matías S/N. Guanajuato, Gto, 36020 México. Guanajuato 36000, México

[2] Facultad de Ciencias Químicas, Universidad de Colima, Km. 9 Carr, Colima-Coquimatlán, 28400, Coquimatlán, Colima, Mexico

[3] School of Resources and Safety Engineering, Wuhan Institute of Technology, Wuhan 430073, Hubei, China

Corresponding author: m.corona@ugto.mx (Mario Alberto Corona-Arroyo)

Abstract: The individual and combined depressive action of metabisulfite and dextrin on pyrite in the presence and absence of amyl xanthate has been studied through contact angle, zeta potential, microflotation, and IR spectroscopy analyses. The combined application of depressants significantly reduces the contact angle of pyrite compared with that of galena, with this effect being enhanced when the pulp is oxygenated during conditioning with metabisulfite, facilitating pyrite surface oxidation. Zeta potential measurements demonstrate the role of the oxidation process in decreasing the magnitude of the negative electric charge on the pyrite surface. These results were further corroborated by IR spectroscopy studies, which confirmed the oxidation of the pyrite surface in the presence of metabisulfite, as well as the co-adsorption of dextrin and amyl xanthate. In microflotation experiments, pyrite and galena exhibited contrasting flotation behaviors, with pyrite being effectively depressed at pH 8 when a combination of air, metabisulfite, and dextrin was used.

Keywords: pyrite, depressant, flotation, dextrin, sodium metabisulfite

1. Introduction

Pyrite is the most abundant iron sulfide mineral in the Earth's crust and is commonly associated as gangue with base metal minerals such as chalcopyrite ($CuFeS_2$), galena (PbS), and sphalerite (ZnS). In most galena-pyrite flotation circuits, sodium cyanide is used with lime as a pH regulator, and the dosages depend on the iron (Fe) grade in the process feed. Lead flotation is conducted within a pH range of 8 to 11.5 (Bulatovic, 2007). For example, Heydari et al. (2019) used a mixture of potassium permanganate and dextrin to depress pyrite during the flotation of galena and sphalerite. This approach enabled effective separation at a pH of 8.5 for galena and 12 for sphalerite. In addition, sodium cyanide is very effective because it can form an insoluble iron cyanide complex that inhibits the electrochemical oxidation of xanthate and consequently the pyrite depression (Wang et al., 2020).

Nevertheless, in response to environmental constraints, researchers have explored alternative solutions, including organic depressants or biopolymers similar to dextrin (DX) (which include substances such as starch, carboxymethylcellulose, and chitosan), polyacrylamides (PAMs), and wood extracts such as lignosulfonates (Bulut et al., 2011; Mu et al., 2016a). Recently, (Zhai et al., (2025) reported an effective separation of pyrite and galena using pullulan polysaccharide (PP) at a pH of 8. Characterization results indicated that the Fe sites in pyrite were more prone to forming stable coordination bonds with the O atoms in the C−O−H groups of PP. In the flotation system of binary minerals, the selective separation of pyrite and galena is considerably improved at pH=8.00 with the introduction of 40 mg/L PP, corresponding to a galena recovery of as high as 91.55 %. Despite their eco-friendliness, these substitutes have not fully supplanted the cyanide-lime combination.

DOI: 10.37190/ppmp/197068

As a result, studies have been conducted to improve the depression efficiency of these reagents. For example, Laskowski et al. (1991) and López-Valdivieso et al. (2004) investigated the intricate interactions among polysaccharides such as dextrin and starch and those between oxides and sulfide minerals. In the adsorption process, dextrin forms complexes via its OH- groups with metallic sites on mineral surfaces. This specific phenomenon is particularly notable in pyrites that contain ferric oxyhydroxide (FeOOH) species from the oxidation processes on the pyrite surface.

Moreover, recent findings confirmed that biopolymer adsorption was augmented with mineral surface oxidation (Mu et al., 2016b, 2015; Mu and Peng, 2019), which highlights its importance in effectively utilizing these reagents. For example, López-Valdivieso et al. (2018) conducted dextrin adsorption experiments on air-oxidized pyrite (30 and 24 hours with air) and showed that maximum adsorption occurred at pH values near the isoelectric point of iron hydroxide (pHiep = 7.5), which forms during the oxidation process. The oxidation times used in their study were 30 minutes and 24 hours, demonstrating the impact of oxidation duration on adsorption behavior. Further insights from Feng et al. (2020) elucidate the efficacy of the hydrogen peroxide oxidation of sphalerite in relation to Locust bean Gum adsorption. Their study concluded that the Gum adsorption onto sphalerite primarily occurred through chemical interactions with oxidation products on the sphalerite surface. However, the combined use of oxidants with organic depressants for galena-pyrite separation remains underexplored. Wang et al. (2020) assessed the combination of calcium hypochlorite ($Ca(ClO)_2$) with dextrin for pyrite depression. Their results indicated that the combined effect of $Ca(ClO)_2$ and dextrin significantly inhibited pyrite flotation in a more efficient manner than their individual effects, particularly in the presence of galena.

For several years, sodium metabisulfite (MBS) has been successful in treating pyrite depression (Dávila-Pulido et al., 2011). In addition, MBS can act as a surface oxidant for pyrite (Mu and Peng, 2019). Shen et al. (2001) used MBS to effectively separate pyrite from sphalerite and mentioned that this separation was achieved because of the oxidation products of pyrite. In a recent study by Liu et al. (2020), sodium sulfite was used with a lignosulfonate biopolymer to improve the separation between chalcopyrite and galena. They reported that sodium sulfite promoted the oxidation of galena and increased the adsorption of the biopolymer because of surface oxidation.

The depression of pyrite has been previously evaluated using either sodium metabisulfite or dextrin individually; however, the combined effect of these reagents has not been reported. In this study, we investigate the joint depressing effect of sodium metabisulfite and dextrin on pyrite flotation using contact angle measurements, zeta potential analysis, microflotation tests, and IR spectroscopy. Additionally, contact angle and microflotation results for galena are presented as a comparison with pyrite.

2. Materials and methods

2.1. Materials

Natural samples of pyrite from Guanajuato, Mexico and galena from Ward's Natural Science Establishment, Inc., USA, and the state of Durango, Mexico were used in this research. The large pieces were manually crushed, and an optical microscope was used to eliminate or remove impurities from the mineral sample. Three types of samples were used: 1-cm^2 crystals for the contact angle measurements, -75 + 53μm fractions for the microflotation studies, and -20 μm fractions for the zeta potential measurements. The samples were characterized using X-ray diffraction (XRD) and chemical analysis via atomic absorption to determine their purity. Fig. 1 shows the diffraction patterns. The chemical analyses revealed 85.9 % Pb and 45.11 % Fe to obtain a concentration of 99.19 % galena and 97.22% pyrite, respectively. The diffraction patterns only show the characteristic peaks of galena and pyrite. No other mineral phase was identified.

It is important to note that the pyrite sample used in this study was prepared in an open atmosphere, which likely resulted in surface oxidation (Wang, 1996). This oxidation may affect the interaction with flotation reagents and may not represent the behavior of fresh, unoxidized pyrite typically found in real ore deposits. Future studies should investigate the effects of using unoxidized pyrite to better understand the implications for flotation performance in natural ore conditions.

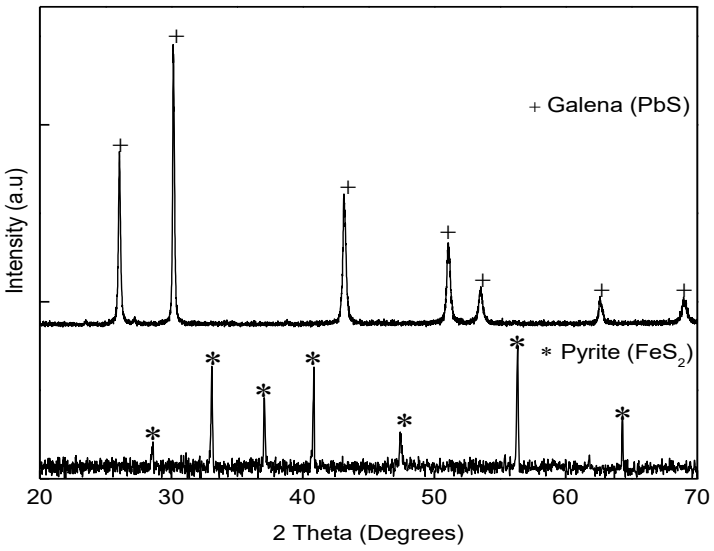

Fig. 1. XRD patterns of galena (top) (+ PDF:00-001-0880) and (bottom)pyrite (*PDF:01-071-1680)

Industrial-grade potassium amyl xanthate (PAX) with a purity of 94% was used as a collector for pyrite and galena without prior purification. Tapioca Dextrin 12 from Stanley Manufacturing Company was used and has been reported (Nyamekye and Laskowski, 1993) to have a molecular weight of 56,000 uma. Sodium metabisulfite from J.T. Baker was used as a depressant. All experiments were performed at a constant ionic strength of $1x10^{-3}$ M NaCl. The water had a resistivity of 18.25 MΩ·cm, and the pH value was adjusted with dilute solutions of NaOH and HCl.

2.2. Contact angle tests

Contact angle studies on pyrite and galena in the presence of dextrin and sodium metabisulfite were conducted by mounting mineral crystals in epoxy resin, polishing them with silicon carbide sandpaper with different grit sizes (#240, #600, #800, #1000, #3000, and #5000) and subsequently polishing them with 0.25 μm alumina powder until a mirror finish was achieved. The crystals were sonicated for 5 minutes to remove any reactive or contaminant particles that could interfere with the contact angle measurement. Then, the samples were conditioned in an aqueous solution to the desired chemical conditions for a specific time (3-10 min). In this study, the individual effects of adding MBS and DX, the effects of pulp aeration in the presence of MBS to enhance the oxidation effect, and the combined effects of the two depressants were evaluated. The pulp pH value was adjusted to 8 by adding aqueous solutions of HCl and NaOH. Then, MBS or DX depressant was added and allowed to contact the mixture for 10 minutes. When both depressants were used, the sample was always first conditioned with MBS and subsequently with DX. Afterwards, PAX was added at the desired concentration, and the mixture was allowed to react for 5 minutes. Conditioning was conducted in a glass cell, and a 1-mm bubble was placed using a Hamilton 0.10-ml microsyringe series 700 with a hook shape. The shadow of the bubble in equilibrium with the crystal and aqueous solution was photographed and processed with the image analyzer (ImageJ) and Contact-Angle plugin (Brugnara, 2006) to obtain the contact angle. Three bubbles were placed for each measurement, and the average angle was reported as the final measurement.

2.3. Microflotation tests

The microflotation studies were conducted using a Hallimond tube (Fuerstenau, 1957). One gram of pyrite or galena at a size of -75 + 53 μm was used in a suspension of 100 ml of deionized water. The minerals were conditioned following a similar sequence of reagent addition to that in the contact angle tests, i.e., the depressants were added before the collector. After the conditioning time ended, the particles were transferred to the flotation tube and floated for 1 minute with a constant high-purity nitrogen flow of 30 mL/min (López-Valdivieso et al., 2006, 2005). After the test, the floatability was calculated by the weight difference. Each flotation test was repeated three times.

2.4. Zeta potential measurements

The interaction mechanism among MBS, DX, and PAX on the pyrite surface was investigated through the zeta potential analysis using a zetameter (Zeta-Meter System 3.0+, USA). This instrument measures the electrokinetic mobility of individual particles through a microscope and converts this mobility into the zeta potential via Smoluchowski equation (Adamson and Gast, 1997). The Smoluchowski's equation, shows the relation between zeta potential and electrophoretic mobility,

$$\zeta = \frac{4\pi\eta}{\varepsilon} U \quad (1)$$

where ζ is zeta potential, U is electrophoretic mobility, η the viscosity of the water, ε the dielectric constant and π the constant. All measurements were conducted at room temperature (25 ± 1 °C) with a constant NaCl concentration of $1x10^{-3}$ M. Five milligrams of pyrite with a particle size of -20 μm was used in a magnetically stirred suspension (100 mL) in the presence of air flow and MBS. The pH of the suspension was measured, and the suspension of particles was subjected to ultrasonic treatment for 5 minutes before the zeta potential test. The supernatant that contained the fine mineral particles was transferred to a capillary cell for the zeta potential measurements. The average of 10 measurements was taken to represent the measured zeta potential (Chen et al., 2023; Demirbas et al., 2007).

2.5. Infrared spectra analysis

ATR-IR studies were conducted to analyze the infrared spectra of pyrite and its interaction products with MBS, DX, and PAX. The measurements were performed using a Perkin Elmer Spectrum 100 Analyzer, covering a range of 600–4000 cm^{-1}. Spectra were acquired with an average of 32 scans at a resolution of 4 cm^{-1}. Samples were ground to a particle size of less than 20 μm and prepared similarly to those used in zeta potential measurements and microflotation. After the designated conditioning time, the particles were filtered and dried at 40°C.

3. Results and discussion

3.1. Contact angle between pyrite and galena

Fig. 2 shows the contact angle as a function of MBS addition (Fig. 2a) and DX addition (Fig. 2b) without the presence of a collector. In the absence of the depressant, the natural contact angle of the minerals is measured, which corresponds to the highest value and subsequently decreases as the MBS/DX dosage increases. It is important to note that contact angle values close to 60°, obtained using the captive bubble technique, indicate that the mineral is considered hydrophobic. In this study, the measured contact angles for galena and pyrite fall within this range, classifying these minerals as partially hydrophobic.The contact angle of pyrite decreases in the presence of MBS from 55° to 42° when it reaches the maximum dosage. Similarly, pyrite in the presence of dextrin has a maximum reduction of 29° with 300 mg/L DX, so DX is slightly more effective in reducing the hydrophobicity of pyrite than MBS. Additionally, these Figs. show that the contact angle of galena slightly decreased in the presence of both MBS and DX, although their effect at these concentrations was minimal

The difference in wettability between galena and pyrite caused by individual depressants is not large, so it is expected that the differences in floatability will not be large. Therefore, the combined effect of the two reagents was evaluated using constant MBS concentrations with and without pulp aeration (150 mL/min of air). The combined effect of the depressants (Fig. 2c) caused a larger reduction of the contact angle than when the depressants were used (Figs. 2a, b) individually. The contact angle of pyrite significant decreases 29° with 60 mg/L dextrin in the presence of MBS. The decrease in contact angle was more effective when pulp preaeration was performed before and during conditioning with MBS. The contact angle value for pyrite crystals at 10 mg/L DX was 18°.

These results highlight the crucial role of oxygen in reacting with MBS. Previous studies (Brandt and Eldik, 1995; Mu and Peng, 2019) have suggested that this reaction leads to the formation of the peroxymonosulfate radical (SO_5^{*-}), a powerful oxidant, which in turn promotes the formation of oxidized species on the mineral surface. These results are consistent with those reported by López-Valdivieso et al. (2018), where dextrin adsorption on the surface of pyrite is promoted by the formation of ferric hydroxide, which plays a key role in the depression of pyrite. The ferric hydroxide forms due

to the oxidation of the pyrite surface facilitated by the presence of oxygen and MBS (Dávila-Pulido et al., 2011).

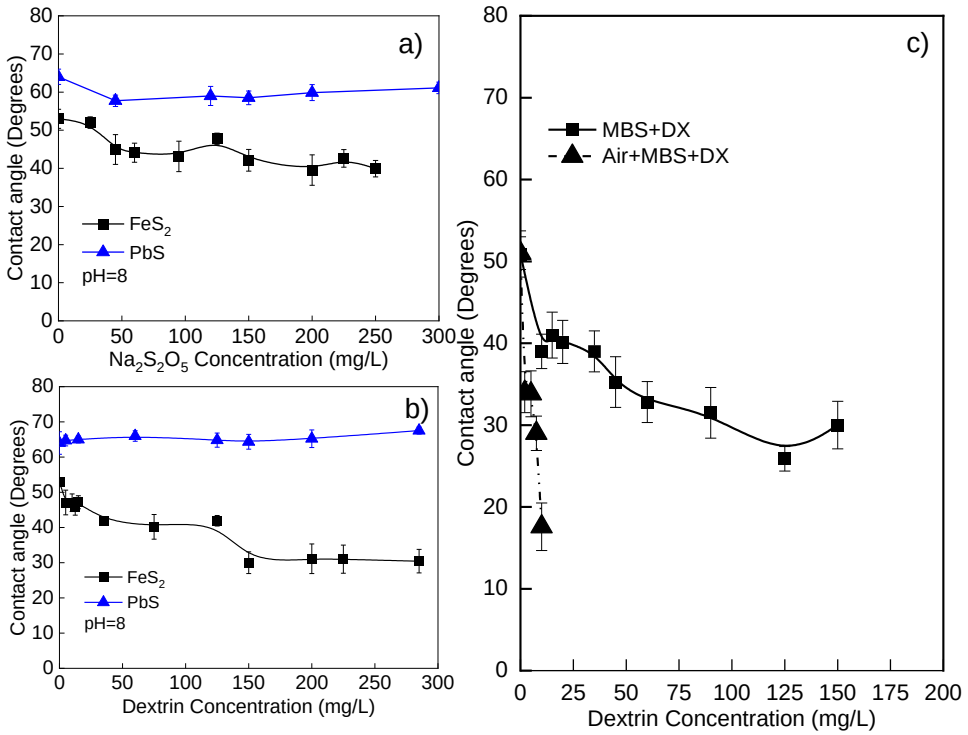

Fig. 2. Contact angle of pyrite and galena as a function of the (a) MBS and (b) DX concentrations at pH 8 without a collector. (c) Contact angle of pyrite as a function of the combination of MBS (150 mg/L) and DX with and without pulp pre-aeration (150 mL/min) and without a collector

In Fig. 3, the effect of adding air + MBS + DX was evaluated in the presence of $1x10^{-3}$ M PAX as a collector. Galena maintained a consistently high contact angle across the entire range of MBS and DX concentrations. In contrast, pyrite's contact angle decreased to 36° with the addition of 10 mg/L DX, indicating a potential for effective separation in the presence of PAX. Furthermore, a reversible change in the contact angle was observed, although this reversibility diminished as the MBS concentration increased, with the effect being less pronounced at 1000 mg/L MBS. A similar phenomenon of contact angle reversibility was previously reported for sphalerite when MBS was used as a depressant (Dávila-Pulido et al., 2011).

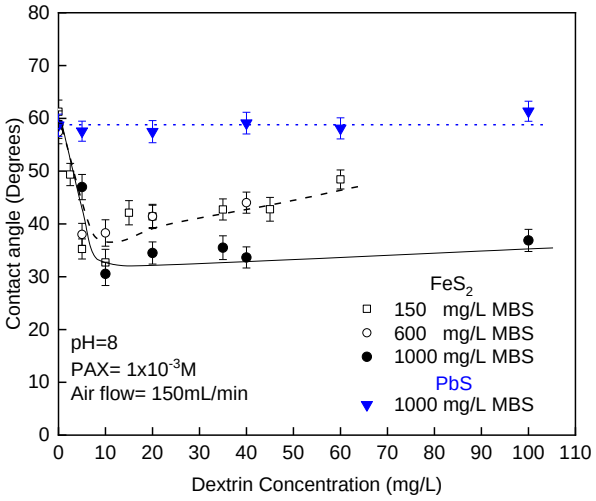

Fig. 3. Contact angles of pyrite and galena with the combination of MBS and DX with preaeration at different MBS concentrations and in the presence of $1x10^{-3}$ M PAX

3.2. Microflotation

Figs. 4a and b show the flotation performance of pyrite and galena as a function of DX and MBS addition in the presence of PAX, respectively. Galena and pyrite exhibited good flotation performance throughout the range of studied dosages because the hydrophobicity established by PAX could not be inhibited by the addition of individual depressants. Fig. 4c shows the effects of using a constant concentration of 150 mg/L MBS and pulp aeration. Pyrite exhibited a decrease in flotation to a value of 46% with a concentration of 25 mg/L DX, demonstrating a selective depressive effect on pyrite while preserving the floatability of galena under these conditions. In addition, pyrite flotation is restored at dextrin dosages above 25 mg/L. This behavior is similar to that reported in contact angle measurement tests. This behavior is likely attributed to the formation of a hydrophobic precipitate involving Fe^{2+} and Fe^{3+} ions, which are released during pyrite oxidation with metabisulfite and react with dextrin and xanthate. According to Liu and Laskowski (1989) and Rath et al. (2000), dextrin preferentially forms precipitates with iron ions at a pH of 8.5. This precipitate can modify the pyrite surface, impacting both contact angle (Fig. 3) and flotation. The reversibility of these effects is observed only in the presence of PAX, which may interact with or alter the precipitate layer. Further coprecipitation tests with PAX would be required to confirm this process but were beyond the scope of this study. Some authors reported good pyrite depression efficiency at low dextrin concentrations of 10-30 mg/L (Wang et al., 2020). However, these differences are attributed to the concentration and type of collector, particularly in this research, which used PAX, which is the most powerful collector among all the xanthates.

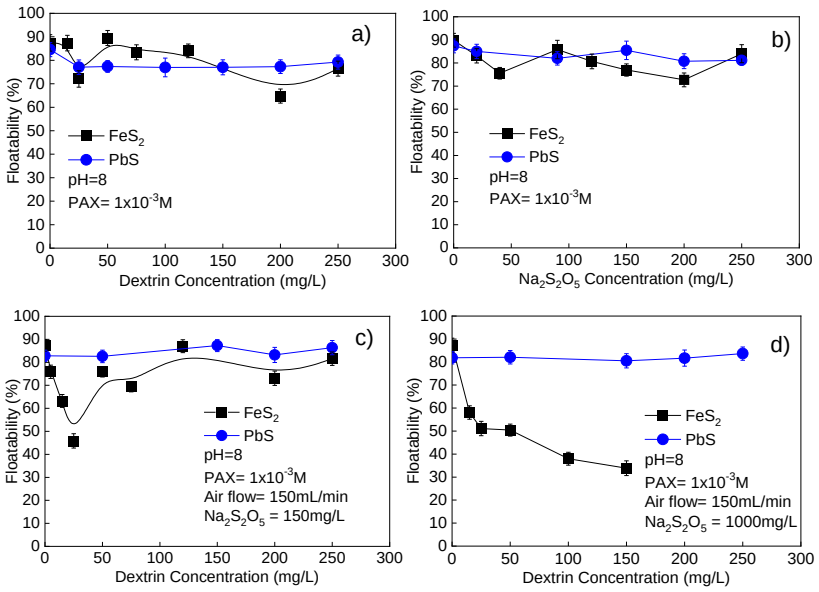

Fig. 4. Microflotation of pyrite and galena as a function of the (a) DX concentration and (b) MBS at pH 8 in the presence of 1x10-3 M PAX. Floatability of pyrite and galena as a function of the DX concentration at 150 (c) and 1000 (d) mg/L MBS with pre-aeration of the pulp (150 mL/min of air) in the presence of 1x10-3 M PAX

As shown in Fig. 4d, at a constant concentration of 1000 mg/L MBS and pulp oxygenation, the combined effect of the depressants considerably reduced the floatability of pyrite, which enables selective flotation between pyrite and galena. The wettability and microflotation test results show that pulp oxygenation during the action of MBS is particularly important so that MBS can function as an oxidant. Some authors (Dávila-Pulido et al., 2011; Mu et al., 2016a) explain that MBS can oxidize the surface of pyrite by forming sulfuric acid and sulfur dioxide.

The dissociation of MBS in water proceeds in two primary steps. First, MBS dissolves and dissociates into disulfite ions ($S_2O_5^{-2}$). In the second step, the disulfite ions undergo hydrolysis, reacting with water to form bisulfite (HSO_3^-) and sulfite (SO_3^{-2}) ions.

The overall process can be summarized as:

$$S_2O_5^{-2} + H_2O = 2HSO_3^- \quad (2)$$

$$HSO_3^- = H^+ + SO_3^{-2} \quad (3)$$

In aqueous solution, sodium metabisulfite thus dissociates into bisulfite and sulfite ions, which may further interact with the medium depending on the pH of the solution

$$S_2O_5^{-2} + 2OH^- = 2SO_3^{-2} + H_2O \quad (4)$$

Moreover, the addition of oxygen to the system can enhance the oxidation of the pyrite surface by MBS because the oxidation of MBS with pyrite is catalyzed by oxygen. It has been reported that the sulfite ion oxidizes to sulfate (reactions 5), and there are intermediate propagation reactions where oxidizing radicals are formed (reactions 5-6), as suggested by Connick et al. (1995) and Mu et al. (2019).

$$SO_3^{2-} + \frac{1}{2}O_{2(ac)} = SO_4^{2-} \quad (5)$$

$$SO_3^{*-} + O_{2(ac)} \rightarrow SO_5^{*-} \quad 6)$$

$$SO_5^{*-} + SO_3^{2-} \rightarrow SO_5^{2-} + SO_3^{*-} \quad (7)$$

When pyrite is oxidized in the presence of sulfite ions SO_3^{2-} and oxygen, the process becomes more complex than a simple reaction with oxygen and water. Sulfite acts as a reducing agent, facilitating the oxidation of sulfur in pyrite and accelerating the release of sulfur products. The main reactions involve the oxidation of pyrite to produce ferrous ion (Fe^{2+}) and sulfate ions (SO_4^{2-}) (Equation 8) followed by the oxidation of ferrous ions to ferric ions (Fe^{3+}), which can further catalyze the oxidation of more pyrite.

$$FeS_2 + 4SO_3^{2-} + 5\frac{1}{2}O_2 + H_2O = Fe^{2+} + 6SO_4^{2-} + 2H^+ \quad (8)$$

The presence of sulfite not only converts to sulfate but also acts as a catalyst. In the oxidation process of ferrous ions (Fe^{2+}) on the pyrite surface, the formation of ferric hydroxide $Fe(OH)_3$ can occur, among other products.

3.3. Zeta potential analysis

The zeta potential of pyrite was determined to investigate the effect of oxidation induced by sodium metabisulfite in combination with aeration. Fig. 5 shows the zeta potential of pyrite as a function of pH with and without 400 mg/L MBS. The isoelectric point (IEP) of pyrite is approximately 6.7, which is consistent with the findings of Jiang et al. (2000), who noted this characteristic behavior of partially oxidized pyrite exposed to the atmosphere (Fornasiero et al., 1992; Jiang et al., 2000; Paredes et al., 2019). With the addition of sodium metabisulfite, the zeta potential becomes negative across the entire pH range, which suggests a significant alteration in the surface electrical properties of pyrite, indicative of the adsorption of SO_3^{2-} and HSO_3^- ions. This adsorption is primarily driven by electrostatic interactions with the positively charged sites on the pyrite surface, as well as specific chemical adsorption mechanisms. The latter involves hydrogen bonding between the sulfite ions and the hydroxyl groups (OH) on the pyrite surface. In particular, this interaction can occur between the proton of HSO_3^- and the surface OH groups, or between the oxygen atoms of SO_3^{2-} and HSO_3^- and the OH groups. This is further supported by the absence of an isoelectric point (IEP) for pyrite in the pH range investigated, which emphasizes the role of specific adsorption mechanisms such as hydrogen bonding.

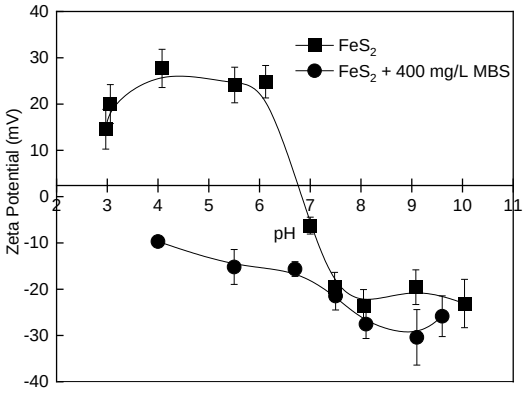

Fig. 5. Zeta potential of pyrite as a function of pH with and without 400 mg/L MBS

Fig. 6 shows that after pyrite particles had been conditioned at pH 8 with airflow for different time intervals, the zeta potential became less negative (inset of Fig. 6). This reduction in negativity is directly related to the surface oxidation of pyrite, which leads to the formation of ferric hydroxide on the mineral surface. It is important to note that the surface oxidation of pyrite occurs unevenly, often manifesting as patches due to variations in the surface structure and reactivity of different crystallographic facets (Chandra and Gerson, 2011; Chernyshova, 2003).

Paredes et al. (2019) conducted zeta potential studies and found that the stable phases that formed during oxidation included ferric oxyhydroxides such as Fe(O)OH, and goethite was one of the thermodynamically most stable forms. Niu et al. (2019) conducted XPS studies and reported that the oxidized species formed on pyrite were SO_4^{2-} and Fe(O)OH.

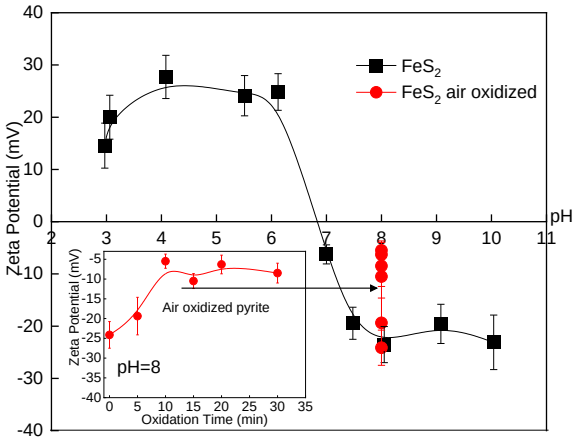

Fig. 6. Zeta potential of pyrite during the oxidation process as a function of the oxidation time with air at a constant pH of 8

Fig. 7 presents the zeta potential of pyrite as a function of the air + MBS addition, which is similar to the conditioning in the contact angle and microflotation measurements. For MBS dosages below 100 mg/L and 5 min of conditioning with air, the zeta potential decreases from -20 to -12.5 mV, which can be attributed to the oxidation process (Fig. 6). When the concentration exceeds 150 mg/L, the zeta potential of pyrite becomes more negative because of the adsorption process of sulfite ions on the oxidized sites and virgin sites, as demonstrated in Fig. 5.

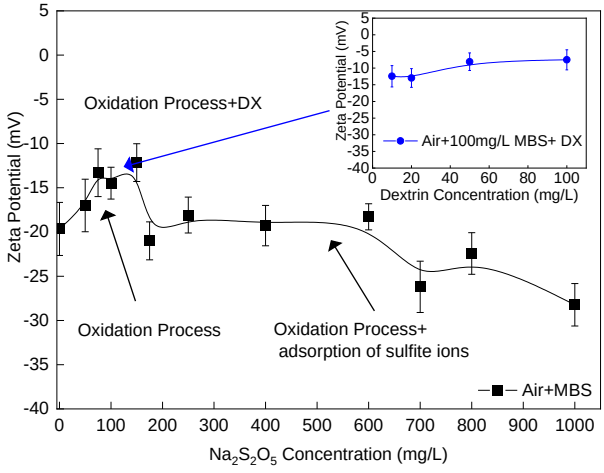

Fig. 7. Zeta potential of pyrite as a function of the MBS concentration; the sample was conditioned 5 min with an air flow of 150 mL/min at pH 8

After the oxidation process (5 min with air +100 mg/L of MBS), various dextrin concentrations were evaluated to determine their adsorption on the oxidized surface. The inset in Fig. 7 illustrates the decrease in zeta potential with increasing dextrin concentration. As reported in several studies,

including López-Valdivieso et al. (2004) and Liu et al. (2000), the addition of dextrin reduces the zeta potential of minerals like pyrite (Rath et al., 2000), galena, and sphalerite (Rath and Subramanian, 1999; Rath et al., 2000), without shifting the isoelectric point (IEP). This indicates that the primary effect of dextrin is to shift the slipping plane farther from the surface, likely due to the large macromolecule's conformational changes. According to Liu et al. (2000), the adsorption of dextrin on pyrite occurs primarily through hydrogen bonding and van der Waals interactions. At pH levels around 8, dextrin behaves as a nonionic polymer, adsorbing onto the pyrite surface without significantly altering its isoelectric point (IEP).

Fig. 8 shows the zeta potential of pyrite vs. pH under various conditions: in the presence of air, 400 mg/L MBS, 100 mg/L DX, and 1x10^{-3} M PAX. Raw pyrite data are included for comparison. Pyrite treated with MBS and DX has a different isoelectric point from that of pure pyrite (Fig. 5) and lower electrical potentials due to the presence of MBS and DX. However, the addition of the collector PAX induces a significant change: the electrical potential becomes negative in the pH range of 3-7, which makes the isoelectric point of oxidized pyrite disappear. Fuerstenau et al. (1990b) and López-Valdivieso et al. (2005) reported that xanthate adsorbed onto oxidized pyrite, formed dixanthogen, and reduced the amount of ferric hydroxide. The zeta potential measurements are consistent with the adsorption and Raman spectroscopy studies by López-Valdivieso et al. (2018), where a co-adsorption of dextrin and xanthate was observed. The combination of MBS and air promotes rapid pyrite oxidation by facilitating surface conditions that increase dextrin adsorption, which does not inhibit xanthate adsorption. These results align with contact angle and microflotation results. Furthermore, López-Valdivieso et al. (2018) demonstrated that under oxidizing conditions, co-adsorption of dextrin and xanthate on pyrite occurs, without hindering xanthate adsorption even in the presence of MBS and air. This co-adsorption is reflected in the shift to more negative zeta potential values upon PAX addition, indicating xanthate adsorption. However, the oxidizing conditions promoted by MBS and air enhance dextrin adsorption, maintaining its role as a depressant, consistent with the contact angle and microflotation results.

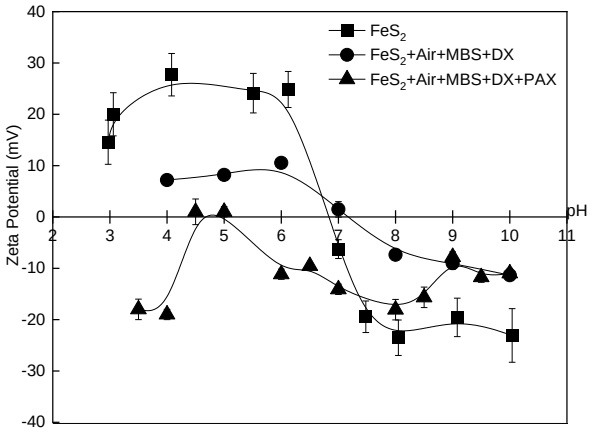

Fig. 8. Zeta potential of pyrite in the presence of air (5 min), 400 mg/L MBS, and 100 mg/L DX + 1x10^{-3} M PAX as a function of pH

3.3. Infrared (IR) spectroscopy analysis of the pyrite surface

Fig. 9a displays the spectra of pyrite exposed to air, MBS, DX, and PAX at pH 8. The IR spectrum of ground pyrite exhibits two wide bands linked to oxidation products on the surface. Zone 1 is located at 1123 cm^{-1}, featuring peaks at 1077 and 1035 cm^{-1}, along with a shoulder at 1013 cm^{-1}. Zone 2 reveals two bands within the range of 661 to 815 cm^{-1}. According to Rath et al. (2000) these two regions are characteristic of pyrite prepared in an open-air environment. The absorption bands in the 1123-1035 cm^{-1} range are attributed to iron sulfate, specifically $FeOHSO_4$ (Chernyshova, 2003; Wang, 1996). Weak signals at 815 and 661 cm^{-1} correspond to the formation of iron hydroxy sulfate, $Fe_8O_8(OH)_6SO_4$, and goethite, α-FeOOH, respectively (Reyes et al., 2022).

After conditioning with air and MBS (Fig. 9b), the peak at 1123 cm^{-1} is significantly reduced. This suggests that some of the sulfoxyl species have dissolved into the solution (Wang, 1996). However, the peaks at 815-649 cm^{-1} are more intense, indicating an increase in the oxidation process on the pyrite

surface. This process is consistent with reports from several authors, who have indicated that the use of sulfite ions on iron-containing minerals, such as pyrite, chalcopyrite (Mu and Peng, 2019), and almandine (Kasomo et al., 2020), leads to the formation of a layer of FeOOH(s) and $FeSO_4$ on the surface, as described by equations 7-10. These products have been confirmed through XPS studies.

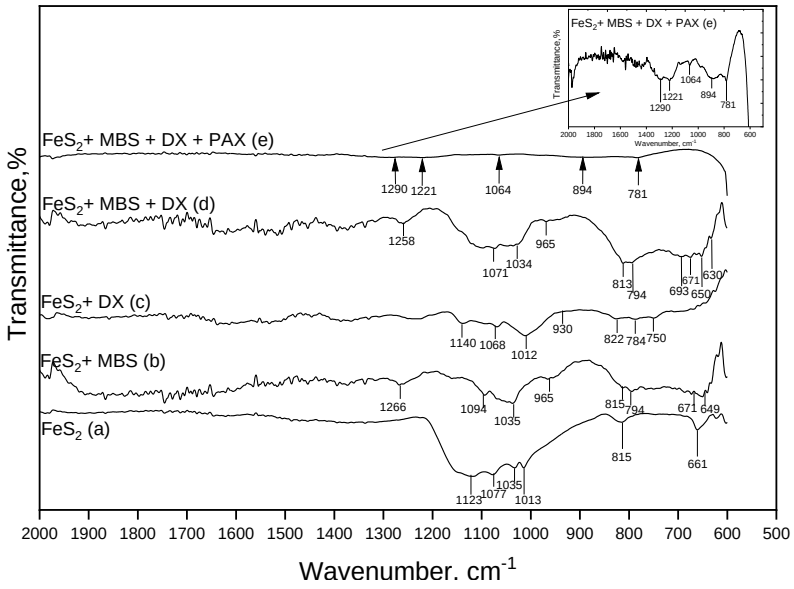

Fig. 9. IR spectroscopy of pyrite before (a) and after the addition of 1000 mg/L MBS (b), 100 mg/L DX (c), 1000 mg/L MBS + 100 mg/L DX (d) and 100 mg/L DX (c), 1000 mg/L MBS + 100 mg/L DX + $1x10^{-3}$ M PAX. All experiments with MBS were conditioned in the presence of air at pH 8. The inset is the same as Fig. 9e but shown at a different scale

The IR spectra of pyrite after interaction with dextrin and air+MBS+DX are depicted in Figs. 10c and 10d, respectively. For dextrin alone, the bands at 1083 and 1021 cm^{-1}, corresponding to the stretching of primary alcohol (–CH_2OH) and CH_2 twisting vibrations, shift slightly to 1084 and 1027 cm^{-1} due to the interaction of the –CO groups with pyrite. Notably, the band around 930 cm^{-1}, present in free polysaccharides, disappears after adsorption onto pyrite, indicating a chemical interaction. Additionally, weak bands near 770 cm^{-1}, attributed to the ring stretching and deformation of β-D-(1–4) and β-D-(1–6) linkages, shift to 784 and 750 cm^{-1} and decrease in intensity after the adsorption of dextrin (Rath et al., 2000).

According to Liu and Laskowski (1989) when there is a higher DX/metal oxide ratio, as observed in oxidized minerals such as galena, pyrite, or sphalerite, the bands at 930 and 760 cm^{-1}, which correspond to the asymmetric and symmetric deformations of the glucose ring, are significantly affected by substitutions on the hydroxyl groups. This is reflected in weak but visible bands, indicating the presence of excess, uncomplexed dextrin. However, when there is an excess of metal oxides, such as iron (FeOOH) in this case, dextrin participates in the reaction, leading to an incomplete spectrum. This phenomenon is observed in Fig. 9d, where the dextrin absorption bands in the 930–760 cm^{-1} region are difficult to distinguish due to the oxidation of pyrite by sodium metabisulfite.

In the air+MBS+DX+PAX pyrite spectrum (Fig. 9e), the intensity of all peaks is reduced, indicating that PAX desorbed some dextrin, and that co-adsorption of PAX and dextrin occurred on the pyrite surface. Moreover, several peaks in the ranges of 1000–1200 cm^{-1} and 500–700 cm^{-1}, which are prominent in the IR spectrum of native pyrite and pyrite+air+MBS, disappeared after the adsorption of xanthate (X^-). This observation aligns with López-Valdivieso et al. (2018), who reported that the redox reaction follows the equation:

$$2\mathrm{Fe(OH)}_3(s,surf) + 2X^- + 6H^+ = X_2(surf) + 2Fe^{2+} + 6H_2O \quad (9)$$

The disappearance of these peaks indicates that the surface of pyrite underwent a redox reaction, consistent with the interaction of xanthate with ferric hydroxide species. In the inset (Fig. 9e), the bands at 1064 cm^{-1} and 781 cm^{-1}, attributed to the adsorption of dextrin, correspond to the stretching of the

primary alcohol (–CH_2OH) and ring stretching, respectively. On the other hand, the bands at 1290 cm^{-1} and 1221 cm^{-1}, associated with dixanthogen, indicate xanthate adsorption. Based on previous analyses, a mechanism for the depression of pyrite by air + MBS + DX in a flotation system with PAX at pH 8 was proposed. Fig. 10b shows that PAX was adsorbed on the surface of pyrite without MBS or DX, which resulted in effective pyrite flotation (Niu et al., 2019). Fig. 10c indicates that pyrite has oxidized patches where a small amount of DX can be adsorbed, in addition to sulfite ion adsorption, which enables partial flotation. When pyrite is first conditioned with MBS in the presence of air, an increase in pyrite oxidation is promoted, which facilitates the adsorption of sulfite ions and greater adsorption of dextrin on these oxidized sites. Thus, pyrite is depressed by increasing the hydrophilicity of its surface, but there is co-adsorption of dextrin and amyl xanthate.

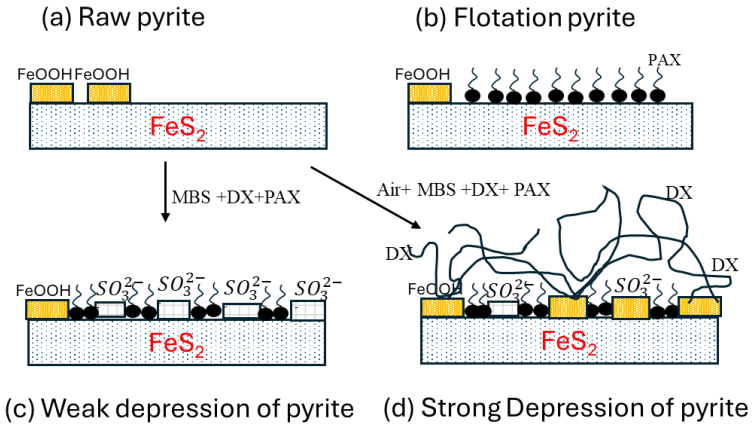

Fig. 10. Depression mechanism of the combination of air + MBS + DX on pyrite

4. Conclusions

In this study, the combined effects of MBS and DX on the hydrophobicity and floatability of pyrite and galena were investigated. The wettability studies revealed that compared to the individual depressant effect, their combined application significantly reduces the contact angles of pyrite and galena, and the contact angle of pyrite is reduced more than that of galena. This effect is notably enhanced when the pulp is oxygenated during conditioning with MBS, which promotes the pyrite surface oxidation.

Zeta potential analysis supports the surface oxidation of pyrite, as evidenced by a decrease in its negative charge. The metabisulfite enhances this oxidation and adsorbs onto the pyrite surface, facilitating DX adsorption and reinforcing pyrite depression.

For effective pyrite depression, the sequence of adding MBS and DX should occur in well-oxygenated conditions to maximize dextrin adsorption and achieve optimal pyrite depression

Infrared spectroscopy studies revealed that, without MBS or DX, PAX adsorbs directly onto the pyrite surface, facilitating flotation. However, conditioning pyrite with MBS in the presence of air promotes oxidation, allowing for enhanced adsorption of sulfite ions and dextrin on oxidized sites.

Acknowledgments

The authors thank the National Council for Science and Technology, México (CONACyT) for the Fellowships 31694 and 31695 to K. Solorzano and C. Echeveste. Additionally, financial support was provided through project A1-S-9361, Universidad de Guanajuato, México. This work is dedicated to the memory of Professor Alejandro López-Valdivieso, whose guidance, wisdom, and unwavering support were instrumental to this research. His legacy continues to inspire and shape our work.

References

ADAMSON, A.W., GAST, A.P., 1967. *Physical chemical of surfaces*. Interscience publishers, New York, 1967.

BRANDT, C., ELDIK, R.V., 1995. *Transition Metal-Catalyzed Oxidation of Sulfur(IV) Oxides. Atmospheric-Relevant Processes and Mechanisms*. Chem. Rev. 95, 119–190.

BRUGNARA, M., 2006. Contact Angle (imagej.net).

BULATOVIC, S.M., 2007. *Handbook of flotation reagents : chemistry, theory and practice : flotation of sulphides ores.* Elsevier Science & Technology Books.

BULUT, G., CEYLAN, A., SOYLU, B., GOKTEPE, F., 2011. *Role of starch and metabisulphite on pure pyrite andpyritic copper ore flotation*. Physicochem. Probl. Miner. Process 48, 39–48.

CHANDRA, A.P., GERSON, A.R., 2011. PYRITE (FES2) OXIDATION: A SUB-MICRON SYNCHROTRON INVESTIGATION OF THE INITIAL STEPS. Geochim. Cosmochim. Acta 75, 6239–6254.

CHEN, D., ARANCIBIA-MIRANDA, N., ESCUDEY, M., FU, J., LU, Q., AMON, C.H., GALATRO, D., GUZMÁN, A.M., 2023. *Nonlinear dependence (on ionic strength, pH) of surface charge density and zeta potential in microchannel electrokinetic flow*. Heliyon 9.

CHERNYSHOVA, I. V., 2003. *An in situ FTIR study of galena and pyrite oxidation in aqueous solution.* J. Electroanal. Chem. 558, 83–98.

CONNICK, R.E., ZHANG, Y.X., LEE, S., ADAMIC, R., CHIENG, P., 1995. *Kinetics and Mechanism of the Oxidation of HSO3− by O2. 1. The Uncatalyzed Reaction*. Inorg. Chem. 34, 4543–4553.

DÁVILA-PULIDO, G.I., URIBE-SALAS, A., ESPINOSA-GÓMEZ, R., 2011. *Comparison of the depressant action of sulfite and metabisulfite for Cu-activated sphalerite*. Int. J. Miner. Process. 101, 71–74.

DEMIRBAŞ, O., ALKAN, M., DOĞAN, M., TURHAN, Y., NAMLI, H., TURAN, P., 2007. *Electrokinetic and adsorption properties of sepiolite modified by 3-aminopropyltriethoxysilanë aminopropyltriethoxysilanë.* Journal of Hazardous Materials. 149, 650-656.

FENG, B., ZHONG, C., ZHANG, L., GUO, Y., WANG, T., HUANG, Z., 2020. *Effect of surface oxidation on the depression of sphalerite by locust bean gum.* Miner. Eng. 146. 106142.

FORNASIERO, D., EIJT, V., RALSTON, J., 1992. *An electrokinetic study of pyrite oxidation.* Colloids and Surfaces 62, 63–73.

FUERSTENAU, D.W., 1957. *Correlation of contact angles, adsorption density, zeta potentials and flotation rate.* Trans. AIME. *208*, 1365-1367.

FUERSTENAU, M.C., NATALIE, C.A.,ROWE, R.M., 1990b. *Xanthate adsorption on selected sulfides in the virtual absence and presence of oxygen, Part 1.* Int. J. Miner. Process. 29, 89–98.

HEYDARI, G., MEHRABANI, J.V., BAGHERI, B., 2019. *Selective separation of galena and sphalerite from pyrite-rich lead-zinc ores: A case study of the Kooshk mine, Central Iran.* Int. J. Min. Geo-Engineering. 53, 43–50.

JIANG, C.L., WANG, X.H., PAREKH, B.K., 2000. *Effect of sodium oleate on inhibiting pyrite oxidation.* Int. J. Miner. Process. 58, 305–318.

KASOMO, R.M., LI, H., CHEN, Q., SORAYA, D.A., LEOPOLD, M., WENG, X., MWANGI, A.D., KIAMBA, E., GE, W., SONG, S., 2020. *Behavior and mechanism of sodium sulfite depression of almandinefrom rutile in flotation system.* Powder Technol. 374, 49–57.

LASKOWSKI, J.S., LIU, Q., BOLIN, N.J., 1991. *Polysaccharides in flotation of sulphides. Part I. Adsorption of polysaccharides onto mineral surfaces.* International Journal of Mineral Processing. 33, 223–234.

LIU, Q., LASKOWSKI, J.S., 1989. *The interactions between dextrin and metal hydroxides in aqueous solutions.* J. Colloid Interface Sci. 130, 101–111.

LIU, M., ZHANG, C., HU, B., SUN, Z., XU, Q., WEN, J., XIAO, J., DONG, Y., GAN, M., SUN, W., ZHU, J., CHEN, D., 2020. *Enhancing flotation separation of chalcopyrite and galena by the surface synergism between sodium sulfite and sodium lignosulfonate*. Appl. Surf. Sci. 507, 145042.

LIU, Q., ZHANG, Y., LASKOWSKI, J.S., 2000. *The adsorption of polysaccharides onto mineral surfaces: An acid/base interaction*. Int. J. Miner. Process. 60, 229–245.

LÓPEZ-VALDIVIESO, A., SÁNCHEZ-LÓPEZ, A.A., PADILLA-ORTEGA, E., ROBLEDO-CABRERA, A., GALVEZ, E., CISTERNAS, L., 2018. *Pyrite depression by dextrin in flotation with xanthates. Adsorption and floatability studies.* Physicochem. Probl. Miner. Process. 54, 1159–1171.

LÓPEZ-VALDIVIESO, A., CERVANTES, T.C., SONG, S., CABRERA, A.., LASKOWSKI, J.S., 2004. *Dextrin as a non-toxic depressant for pyrite in flotation with xanthates as collector*. Miner. Eng. 17, 1001–1006.

LÓPEZ-VALDIVIESO, A., LÓPEZ, A., ESCAMILLA, C., FUERSTENAU, M.C., 2006. *Flotation and depression control of arsenopyrite through pH and pulp redox potential using xanthate as the collector*. Int. J. Miner. Process. 81, 27–34.

LÓPEZ-VALDIVIESO, A., LÓPEZ, A., SONG, S., 2005. *On the cathodic reaction coupled with the oxidation of xanthates at the pyrite/aqueous solution interface.* Int. J. Miner. Process. 77, 154–164.

MU, Y., PENG, Y., 2019. *The role of sodium metabisulphite in depressing pyrite in chalcopyrite flotation using saline water*. Miner. Eng. 142, 105921

MU, Y., PENG, Y., LAUTEN, R.A., 2016a. *The depression of pyrite in selective flotation by different reagent systems – A Literature review*. Miner. Eng. 96-97, 143-156.

MU, Y., PENG, Y., LAUTEN, R.A., 2016b. *The depression of copper-activated pyrite in flotation by biopolymers with different compositions*. Miner. Eng. 96–97, 113–122.

MU, Y., PENG, Y., LAUTEN, R.A., 2015. *Electrochemistry aspects of pyrite in the presence of potassium amyl xanthate and a lignosulfonate-based biopolymer depressant*. Electrochim. Acta. 174, 133–142.

NIU, X., CHEN, J., LI, Y., XIA, L., LI, L., SUN, H., RUAN, R., 2019. *Correlation of surface oxidation with xanthate adsorption and pyrite flotation*. Appl. Surf. Sci. 495, 143411.

NYAMEKYE, G.A., LASKOWSKI, J.S., 1993. *Adsorption and Electrokinetic Studies on the Dextrin-Sulfide Mineral Interactions*. Journal of Colloid and Interface Science. 157 (1993) 160-167.

PAREDES, A., ACUÑA, S.M., GUTIÉRREZ, L., TOLEDO, P.G., 2019. *Zeta potential of pyrite particles in concentrated solutions of monovalent seawater electrolytes and amyl xanthate*. Minerals. 9, 1-12.

RATH, R., SUBRAMANIAN, S., 1999. *Adsorption, electrokinetic and differential flotation studies on sphalerite and galena using dextrin.* Int. J. Miner. Process. 57, 265–283.

RATH, R.K., SUBRAMANIAN, S., PRADEEP, T., 2000. *Surface chemical studies on pyrite in the presence of polysaccharide-based flotation depressants.* J. Colloid Interface Sci. 229, 82–91.

REYES, M., HERRERA, G., ESCUDERO, R., PATIÑO, F., REYES, I.A., FLORES, M., PALACIOS, E.G., JUÁREZ, J., BARRIENTOS, F., 2022. *Surface Spectroscopy of Pyrite Obtained during Grinding and Its Magnetisation.* Minerals. 12, 1444.

SHEN, W.Z., FORNASIERO, D., RALSTON, J., 2001. *Flotation of sphalerite and pyrite in the presence of sodium sulfite.* Int. J. Miner. Process. 63,17-28

WANG, X.-H., 1996. *Interfacial Electrochemistry of Pyrite Oxidation and Flotation.* J. Colloid Interface Sci. 171, 413-428.

WANG, C., LIU, R., AHMED KHOSO, S., LU, H., SUN, W., NI, Z., LYU, F., 2020. *Combined inhibitory effect of calcium hypochlorite and dextrin on flotation behavior of pyrite and galena sulphides*. Miner. Eng. 150.

ZHAI, Q., LIU, R., DONG, W., XIE, Z., SUN, W., 2025. *Separation of galena and pyrite via green organic macromolecules at low alkalinity: Flotation response and surface adsorption mechanisms*. Sep. Purif. Technol. 354, 129240.